Journal of
Synchrotron Radiation

ISSN 0909-0495

Received 25 May 2005
Accepted 2 August 2005

Adapting polychromatic X-ray microdiffraction techniques to high-pressure research: energy scan approach

Gene E. Ice,[a] Przemyslaw Dera,[b]* Wenjun Liu[c] and Ho-kwang Mao[b]

[a]Oak Ridge National Laboratory, PO BOX 2008 MS6118, Oak Ridge, TN 37831-6118, USA, [b]Geophysical Laboratory, Carnegie Institution of Washington, 5251 Broad Branch Road NW, Washington, DC 20015, USA, and [c]UNICAT, Sector 34-ID, APS, Argonne National Laboratory, Argonne, IL 60439, USA. E-mail: p.dera@gl.ciw.edu

Polychromatic single-crystal diffraction (pSXD) offers important advantages compared with monochromatic diffraction, such as ultrafast data collection and the ability to collect diffraction data without sample rotation. Despite the relevance of these advantages for applications in high-pressure experiments, pSXD has never been successfully applied for full structure determination at high pressure. Here the theory of polychromatic microdiffraction, strategies developed to adapt it to high-pressure applications, and results of pilot experiments are described. Special emphasis is placed on experiments with microcrystals and multigrain aggregates, and on the use of monochromator scans to extend the pressure range for single-crystal structure determination to the megabar region. Closely related applications to materials research problems are also discussed.

Keywords: Laue diffraction; high pressure; structure determination.

1. Introduction

Crystallographic information is essential for understanding the physical properties and transformation mechanisms of materials. However, diffraction experiments on high-pressure samples are challenging owing to restrictions imposed by the need for high-pressure environmental chambers, typically diamond anvil cells (DACs). For example, high-pressure diffraction experiments must deal with small sample volume inside a pressure-producing chamber that contributes background and restricts access to reciprocal space. Although synchrotron sources provide the ultra-brilliant X-ray beams needed to study small sample volumes, crystallographic techniques currently used at high-pressure synchrotron beamlines are modifications of standard methods, such as monochromatic powder and single-crystal diffraction, with an emphasis placed on small sample sizes (small beam focal spot). As described below, the conservative use of conventional experimental approaches severely limits the pressures at which full structure determination is possible and new methods are needed, particularly for single-crystal diffraction.

Single-crystal X-ray diffraction (SXD) experiments are uniquely important for high-pressure research, as they provide the most unambiguous structural information for unknown structures. However, while other high-pressure methods typically cover pressures from 0 to 300 GPa (Liu & Vohra, 1996; Mao & Bell, 1978; Mao *et al.*, 1998), SXD is currently limited to much lower pressures owing to the difficulties imposed by a small sample volume in a complex sample chamber. The maximum pressure of published SXD studies with full structural analysis is about 30 GPa (Zhang & Ahsbahs, 1998; Zhang *et al.*, 1998; Kim-Zajonz *et al.*, 1998; Yamanaka *et al.*, 2001). Above 30 GPa, SXD has been used only to determine orientation matrices and unit-cell parameters [*e.g.* stishovite to 65 GPa (Kingma *et al.*, 1995; Mao *et al.*, 1994) and hydrogen to 119 GPa (Loubeyre *et al.*, 1996)]. Because full SXD analysis with structure refinement has not been possible for ultrahigh pressures, research above 30 GPa has relied on powder diffraction and the Rietveld method for structure refinement. These methods cannot match the unambiguous and direct crystal structure determination by SXD.

Besides the ease of interpretation of SXD data, another important argument in favour of single-crystal experiments, especially critical with small sample volumes intrinsic to high-pressure experiments, is the issue of powder statistics. In a powder diffraction experiment, in order to obtain reliable peak intensity information, sufficient number of grains has to be present in the illuminated sample volume. At pressures exceeding 1 Mbar the sample is usually thinner than 0.01 mm, making the powder statistics very poor. With a single-crystal sample, on the other hand, in most cases the specimen can be conveniently polished before the experiment to a thickness of 5 μm, which still provides a satisfactory signal-to-

noise ratio, and allows pressures well in excess of 1 Mbar to be reached.

Structure determination by ultrahigh-pressure SXD has specific requirements that an ideal experimental approach should satisfy: (i) the ability to work with samples in the size range 0.5–10 μm, (ii) the ability to determine unknown lattice parameters, (iii) the ability to minimize, or even avoid, sample rotation during data acquisition, (iv) the ability to retrieve precise structure factor amplitude information covering a sufficient volume of the reciprocal space, and (v) the ability to collect adequate intensity information in a relatively short time, preferably a fraction of a second. Unfortunately, no existing instrument or methodological solution satisfies all of these requirements.

Here, we discuss the adaptation of emerging polychromatic microdiffraction techniques and instrumentation developed for materials research to extend the pressure range for structure determination by single-crystal diffraction. The use of polychromatic microdiffraction for measurements of inhomogeneities of materials is a rapidly developing field with important lessons for high-pressure diffraction. However, whereas the emphasis with materials research has been on understanding mesoscopic defect structures in materials with known crystal structure, in high-pressure research the emphasis is on determining unknown structures and evaluating the electron density distribution within a unit cell. Nevertheless, as described below, polychromatic diffraction can be applied in several ways to achieve the goals of high-pressure research. In this paper we emphasize the use of nondispersive energy scans that map large volumes of reciprocal space.

2. Polychromatic diffraction

With conventional monochromatic single-crystal X-ray diffraction (mSXD), a sample is rotated to multiple orientations to satisfy the Bragg condition for different families of crystallographic planes. The directions and intensities of beams diffracted from the sample are used to determine the crystal structure; the directions of the diffracted beams describe the geometry of the reciprocal space (unit-cell parameters), whereas the distribution of the electron density (atomic positions within the unit cell) can be deduced from the reflection intensities.

Monochromatic SXD experiments are widely used for crystal structure determination because the data interpretation is robust, well developed and, with sufficient data, unequivocal. When working with very small samples and beams, however, rotations can contribute serious problems to the interpretation of measured reflection intensities, as a result of changes in the illuminated volume (Chung & Ice, 1999). Also, the necessity to record multiple images corresponding to different crystal orientations significantly extends the data collection time. Finally, the presence of an environmental chamber may restrict the reflections that can be accessed.

An alternative to an mSXD experiment is a white-beam (polychromatic) experiment that, depending on the choice of detector, can be performed in an energy-dispersive (ED) manner (*e.g.* solid-state detector) or with Laue diffraction (LD) (with an area detector). The ED pSXD approach at high pressure is discussed elsewhere (Dera *et al.*, 2005).

In a LD experiment, the Bragg condition is simultaneously satisfied for many reflections with any crystal orientation, each reflection using a Bragg-condition-satisfying energy component of the incident beam. The fact that no rotation is required simplifies the physical process of data collection, and greatly accelerates data collection time. Modern X-ray optics (*e.g.* Kirkpatrick–Baez focusing mirrors; Ice *et al.*, 2000) can produce intense hard X-ray beams with focal spots of less than 1 μm. If a broad-bandpass white beam is used, even from less-brilliant sources like bending magnets or wigglers, an exposure time for a single Laue image can be well below 1 s, and the primary limitation of the frequency of data collections is imposed by the dead time of the detector.

So far, Laue diffraction has found three major areas of application that significantly benefit from its unique advantages: (i) protein crystallography, in which data quality deterioration owing to sample radiation damage can be minimized by very short irradiation times (*e.g.* Ren *et al.*, 1999), (ii) studies of dynamic processes, in which short data collection time enables time resolution (see *e.g.* Ren & Moffat, 1994), and (iii) polychromatic microdiffraction used in materials science, where avoiding sample rotation and the availability of depth-resolution are critical for resolving mesoscale inhomogeneities (Larson *et al.*, 2002; Chung & Ice, 1999; Tamura *et al.*, 2003). Recently, the LD technique has also been successfully applied to single-crystal time-of-flight neutron diffraction experiments (Cole *et al.*, 2001), allowing for tremendous reduction of the data collection time. Below we briefly review materials science applications that indicate possible directions for high-pressure measurements.

3. Polychromatic microdiffraction for materials science

When only a small number of grains are illuminated by a polychromatic X-ray beam, the Laue patterns from each grain can be distinguished. This has led to the development of a new class of instrumentation called the three-dimensional X-ray crystal microscopes, which use submicrometre X-ray beams to minimize the number of illuminated grains in polycrystalline samples. The basic elements of a three-dimensional X-ray crystal microscope are illustrated in Fig. 1. As shown, a small polychromatic X-ray beam is focused onto a sample and the Laue patterns generated along the beam path are detected by an X-ray-sensitive area detector. The overlapping Laue patterns are resolved by differential aperture microscopy where an absorbing wire is passed near the surface of the sample (Fig. 2, for detailed description see Larson *et al.*, 2002). After reconstruction, the individual Laue patterns from small volume elements along the incident beam path are recovered.

Once the individual Laue patterns are recovered, the key step for many materials studies is to index the patterns in order to determine the local crystal orientation. The main problem with indexing reflections from Laue diffraction is the

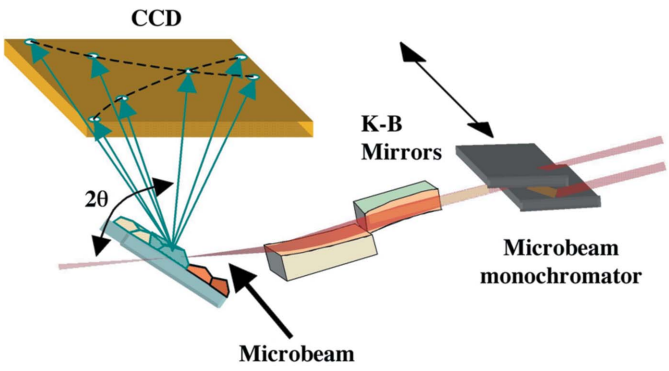

Figure 1
Typical experimental setup for polychromatic microdiffraction measurements in materials science. The intense synchrotron X-ray beam can either be passed directly onto a nondispersive Kirkpatrick–Baez focusing mirror optics or can first be monochromated by a special microbeam monochromator. The overlapping Laue patterns from grains illuminated by the incident beam are detected by an X-ray-sensitive CCD area detector.

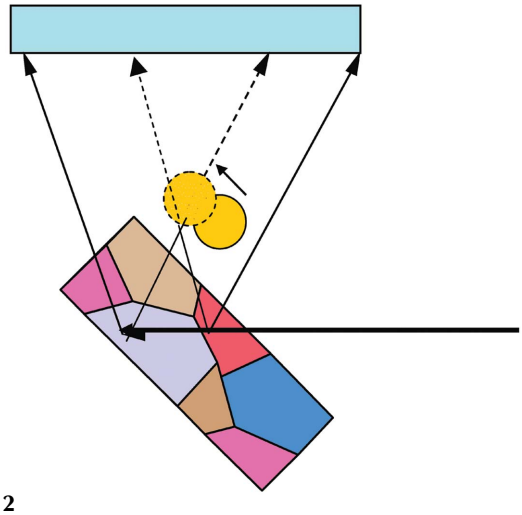

Figure 2
Differential aperture microscopy applied to obtain resolution along the incident X-ray beam in a Laue microdiffraction experiment with a penetrating beam. The position of the movable wire can be precisely calibrated with respect to the detector and the incident X-ray beam. As the wire moves near the sample surface it intercepts X-rays diffracted from the grains in the sample. Changes of the diffracted intensity into each pixel of the detector can be correlated to the wire position and ray-traced back to the intercept with the incident beam. In this way the Laue diffraction pattern from each subgrain volume element along the incident beam path can be determined.

lack of information about their energy; formally a Laue pattern is composed of weighted radial line integrals in reciprocal space and, as a consequence, the length of the reciprocal-space vectors and the relative contribution of orders along the line integral cannot be determined from the Laue pattern alone. Since the *d*-values are not known, the only information that can be used for assigning indices are inter-vector angles. With a sufficient number of observations, however, it is possible to assign indices to the reflections in a LD image without determining absolute values of the unit-cell parameters. A method based on reciprocal space rotation was proposed by Pan (1992). Other methods, developed to deal with this problem, include the gnomic projection approach (Carr *et al.*, 1992), conic recognition (Ravelli *et al.*, 1996), Hough transform (Wenk *et al.*, 1997), the three-dimensional EUCLID generalization method (Sheremetyev & Gorfman, 2001) and inter-vector angle recognition (Chung & Ice, 1999).

Once the Bragg reflections are indexed, the orientation matrix of the crystal can be calculated, and detector coordinates of all the reflections (including those with negligible intensity) can be calculated. For polycrystalline samples, the local distribution of crystal orientations in three-dimensions is determined, and from the distribution of local orientations the dislocation tensor can be calculated. Since the *d*-spacing information is not available, only the unit-cell axial shape (axial ratios and interaxial angles) can be determined.

If the unstrained unit-cell shape for the measured crystal is known, the deviatoric strain (change in unit-cell shape) can be determined, based on the small angular differences in the indexed reflection angles from those expected for an unstrained unit cell. The deviatoric strain tensor is related to the stress tensor through the single-crystal elastic compliance matrix. The information typically recovered therefore includes local crystal orientation distributions, crystalline unit-cell deformation (elastic strain/stress) and the dislocation tensor, which is related to the density of unpaired dislocations.

As illustrated in Fig. 1, it is also possible to include a special nondispersive monochromator to precisely determine the wavelength of individual reflections. The monochromator can be used to scan an energy range near the predicted energy of a Laue reflection. This allows for precise determination of the reciprocal-space vector length, when absolute strain information is needed.

Polychromatic microdiffraction has wide applications for structural characterization of inhomogeneous materials (Ice, Larson *et al.*, 2005). Local structure (of individual micrograins), texture (crystal-orientation), elastic strain and dislocation-tensor distributions can all be nondestructively measured with submicrometre resolution in three-dimensions between and within polycrystalline or single-crystal grains. Although the development of modern polychromatic microdiffraction was originally motivated by the need to understand local stress during electromigration in thin films (Barabash *et al.*, 2004), the few available instruments are overwhelmed with diverse scientific opportunities to study mesoscale (0.1–100 μm) structure and dynamics in a range of materials. Recent measurements have studied the distinct mechanical deformation behavior of grain boundaries in polycrystalline materials (Barabash *et al.*, 2005), the behavior of grain growth both at a surface and in three-dimensions (Budai *et al.*, 2003, 2004), and the redistribution of strain and stress owing to mis-oriented three-dimensional and thin-film grains (Pang *et al.*, 2005).

Experiments to date are just a beginning. The unique instrumentation developed for polychromatic microdiffraction has potential applications to a number of exciting scientific frontiers. Larson *et al.* (2002) demonstrated how monochromatic energy scans can be used to determine the absolute elastic strain tensor (unit-cell volume) of a single crystal. This

prototype measurement of hydrostatic strain followed the three-dimensional *in situ* change in unit-cell volume within a bent single crystal. Other measurements with the three-dimensional X-ray crystal microscope at the APS (Ice, Barabash & Liu, 2005) have demonstrated the ability to determine defect structure in very small single-crystal volumes. These experiments use a monochromator scan through the Bragg energy of a Laue reflection to resolve the three-dimensional Huang scattering near the Laue reflection. The full three-dimensional reciprocal space map around individual Laue spots (Fig. 3) can be used to extract information about the defect content of the crystal. This same approach can be extended to high-pressure research to determine the absolute reflectivity of each reflection, an essential step to determine the electron density map within the unit cell.

4. Polychromatic microdiffraction at high pressure

The ability of polychromatic microdiffraction to determine the crystalline structure of small volumes without sample rotations is a major advantage for high-pressure research. This allows for submicrometre spatial resolution within a relatively large DAC. For high-pressure experiments, the geometry of the experiment is determined by the type of the diamond anvil cell used; a $2\theta \simeq 90^\circ$ reflective geometry is needed for panoramic cells with semi-transparent gasket (usually made of Be or amorphous B) and a transmission geometry is needed for polar cells (Fig. 4).

Regardless of the detector choice and geometry, the presence of a DAC introduces significant difficulties: (i) limited access to reciprocal space; (ii) reflection intensities effected by absorption and extinction; and (iii) limited scattering power and signal-to-noise of very small samples (the ultimate pressure that can be achieved depends on the volume of the sample compressed; smaller volume means higher ultimate pressure). Two problems associated with mSXD are fortunately far less important for pSXD: (i) the need to keep the illuminated volume constant during sample rotations and (ii) the need to maintain hydrostaticity.

Improvement of sample pressure uniformity is another area where polychromatic microdiffraction techniques can be used to advantage. When a quasi-hydrostatic pressure medium is used, the pressure has a distribution within the gasket hole and the incident X-ray beam tends to illuminate the sample through a range of pressures as well. As described above, resolution along an incident polychromatic microbeam can be determined with the use of differential aperture microscopy. The presence of the DAC, however, complicates the straightforward application of differential aperture methods because the aperture wire cannot be passed as close to the sample as is desirable (standard distance is $\sim$0.2 mm). Even with relatively poor differential aperture geometry, a spatial resolution along the incident beam of about 2–5 μm should be possible. This is sufficient to greatly reduce the influence of pressure variations within the cell.

Despite the important information determined from existing polychromatic microdiffraction experiments, standard materials science applications do not routinely recover three important high-pressure characterization parameters: (i) structure as a function of pressure/temperature, (ii) unit-cell volume as a function of pressure/temperature and (iii) structural accommodations to pressure/temperature within the unit cell. Indeed, in most of the materials applications of Laue microdiffraction, the structure is typically assumed to be known for samples under investigation. So far software to automatically detect crystalline phase distributions and determine structures of new polymorphs has not been developed for polychromatic microdiffraction instruments. Even unit-cell volume is not routinely recovered with polychromatic microdiffraction; the additional complexity of determining hydrostatic strain is often not justified for materials research. As a consequence, experimental modifications to materials polychromatic microdiffraction diffraction techniques are essential for high-pressure applications.

5. Reciprocal space access

In structure-determination experiments it is essential to obtain data from a sufficient volume of reciprocal space to properly constrain the electron density maps and the atomic positions within the unit cell. This is especially true for *ab initio* structure determination by direct methods or Patterson analysis. The demand becomes even more critical in the case of structures with low symmetry, large unit cells or when the structure factor amplitude information is not very precise (*e.g.* because of absorption and extinction, as is the case with DAC experiments). Therefore, in all high-pressure experiments aimed at structure determination, a special emphasis must be placed on maximizing the number of observations (accessible volume of reciprocal space).

In the case of polychromatic diffraction from a small fixed sample in a DAC, the geometry of the DAC always restricts access to the detector solid angle [see Finger & King (1978) and Miletich *et al.* (2000) for discussions on the reciprocal space access for mSXD experiments]. In the case of polar DACs the access for incident and diffracted beams is possible within a cone around the cell axis, symmetrically on both sides of the cell, while for panoramic cells the reverse situation is true, and access is available with the exception of the cone around the cell axis. The issue of reciprocal space coverage in pSXD experiments has been discussed by Cruickshank *et al.* (1991). As illustrated in Fig. 5, the volume of reciprocal space viewed by an area detector is much larger for polychromatic microdiffraction in the panoramic geometry than for the polar geometry (in forward-scattering setting). As a result, polychromatic microdiffraction experiments without sample rotation and with the polar geometry are probably only practical for relatively large unit-cell samples with low integrated reflectivity from the reciprocal lattice sites.

6. Reflection energy determination

In order to determine the absolute unit-cell parameters of a crystal, the scattering directions of at least four Laue reflec-

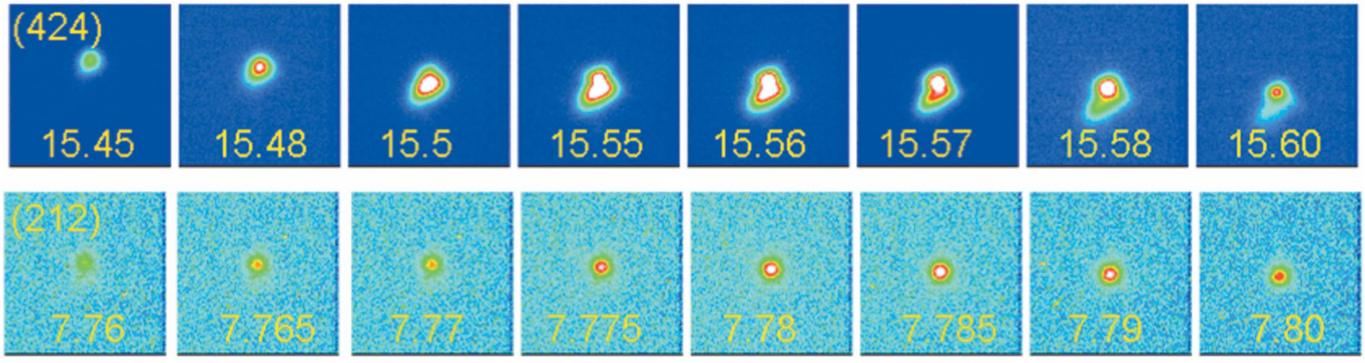

Figure 3
The Huang scattering distribution in reciprocal space near a fundamental (424) or a superstructure (212) reflection from a NiAl superalloy is characterized in this measurement of the diffracted intensity distribution as a function of X-ray energy. The area detector records the diffracted intensity in a spherical shell of reciprocal space whose radius is determined by the X-ray energy. From the Huang scattering it is possible to determine the local strain imposed by a coherent second phase that is distributed inside the super alloy crystal.

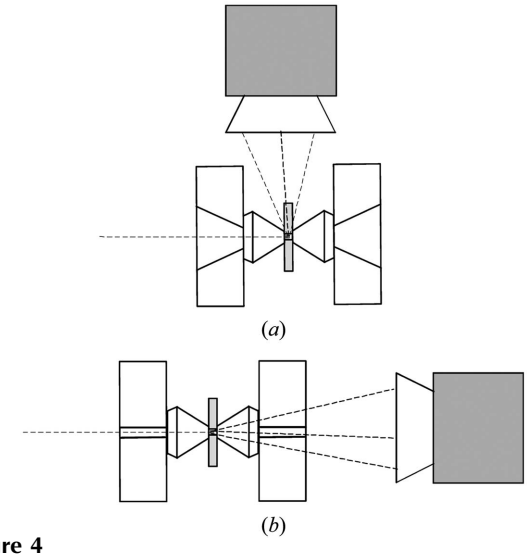

Figure 4
Geometry of the diffraction experiment with area detector (*a*) a panoramic DAC with X-ray transparent gasket and (*b*) a polar cell with nontransparent gasket.

tions must be determined, together with the energy of at least one of the reflections (Chung & Ice, 1999). In addition, to determine the integrated reflectivity of each reciprocal space peak it is essential to separate the contribution to Laue spots arising from different order reflections. Below we review experimental ways of dealing with the problem of unknown spectral distributions corresponding to each reflection in Laue diffraction.

6.1. Monochromatic energy scan

Nondispersive energy scans provide a powerful way to combine most of the advantages of pSXD and mSXD. The heart of this approach is a monochromator design (Fig. 1), which can pass either a white beam or can be inserted into the polychromatic beam and produce monochromatic radiation directed onto the same sample position preserving the path of the original polychromatic beam (Ice *et al.*, 2000). With this monochromator, the incident energy can be scanned to cover

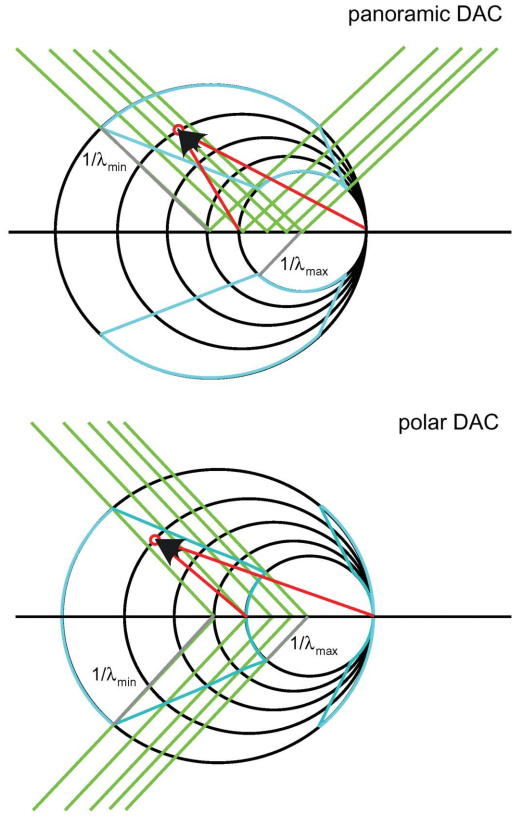

Figure 5
Accessibility of reciprocal space (blue outline) in panoramic and polar DAC. Green lines illustrate the opening cones of the DACs. For the polar DAC, both forward and backward geometries are shown. Note that a much larger volume of reciprocal space is accessed with the panoramic cell, but the integrated reflectivities are lower because of the larger momentum transfer (compared with polar forward geometry).

the whole range or part of the white-beam spectrum. Combined with an X-ray-sensitive area detector, a series of monochromatic images can be collected with varying incident wavelength. The monochromatic image series can then be analyzed to detect 'appearance' and 'disappearance' of reflections as a function of X-ray energy. The reflection energy is determined by fitting the energy profile (integrated intensity

as a function of monochromatic energy), as illustrated in Fig. 6.

Although the monochromator scan technique solves in a very elegant way most of the limitations of Laue diffraction for high-pressure research, it is currently constrained by limitations of detector technology, and is quite time-consuming. In order to accurately evaluate the energy profiles of reflections, small energy steps are needed and, as a consequence, a large number of monochromatic images must be acquired, each of which contains a very small amount of information. With readout times of standard CCD detectors much longer than the typical exposure time, a fine-step energy scan cannot be repeated for high-pressure experiments at each pressure step because of their duration. For example, a rather large energy increment of 10 eV requires 1000 images to cover a 10 keV energy range. With a readout time of about 5 s, this corresponds to a total data collection time of about 1.5 h.

Advanced hardware, software and better integration of the detector can greatly accelerate the data collection time for energy scans. For example, 16-bit 2k × 2k detectors with 20 frames per second readout times are now becoming available. Similarly, if the approximate energies of various reflections can be estimated from rough measurements, then small regions of interest can be selected from the area detector. These regions of interest can be read out orders-of-magnitude faster than the entire CCD. With intelligent software and high-performance hardware it should therefore be possible to make ∼3 eV steps around all reflections in about 5 min. This would allow for full scan measurements as a function of pressure.

6.2. Energy-dispersive detector

Another powerful strategy for the issue of the unknown and overlapping energies is to combine the use of LD with an energy-dispersive detector (EDD), such as a Ge solid-state detector. An EDD is usually a point detector, which determines the spectral distribution of intercepted diffraction. Once the Laue pattern is collected from the sample and indexed, the angles of all the observed reflections in the Laue pattern can be calculated. In order to determine the energies corresponding to each reflection, it is enough to position the detector in a way that intercepts a diffracted beam and collects the energy spectrum. Precise centering of the reflection with the use of EDD is not usually necessary as long as the reflection is not near the edge of the detector. Multiple reciprocal vectors along the same radial line are automatically resolved which allows for determination of the integrated reflectivity in addition to the vector length. The details of this approach are discussed elsewhere (Dera *et al.*, 2005). This method can be very fast for measuring absolute unit-cell dimensions and relatively fast for measuring integrated reflectivities of several reflections.

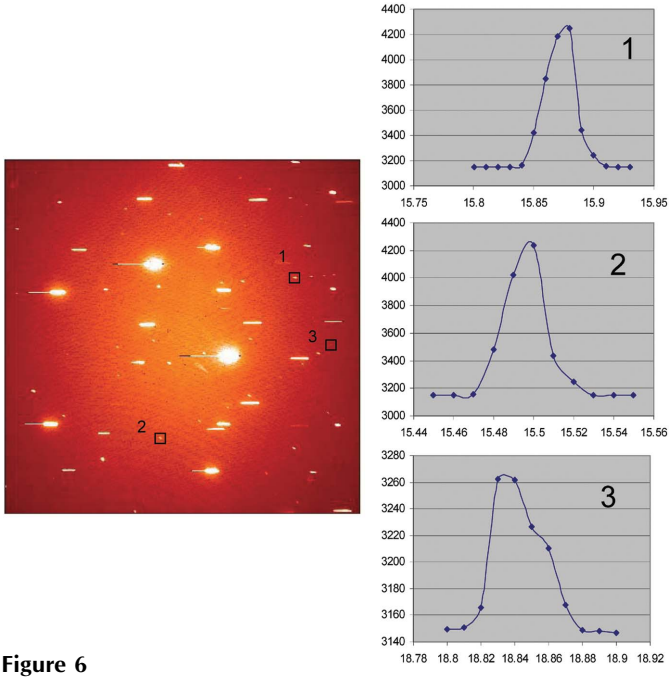

Figure 6
Energy profiles of selected reflections.

6.3. Foil-mask spectroscopy

An alternative solution to approximately determining energies of peaks draws on the energy-dependence of the X-ray attenuation coefficient of metal foils, and utilizes measured values of relative transmission with and without the foil present in the incident beam to estimate the reflection energy. The foil-mask spectrometry method was implemented and tested by Hanley *et al.* (1996, 1997). This method is conceptually analogous with the technique of stacking numerous photographic emulsion sheets on top each other, exposing them and then extracting energy data by determining how many sheets the X-ray photons penetrate (blacken). This approach should be able to resolve energies with ∼30 to 50 eV precision. Although the foil-mask spectrometer approach does not match the energy resolutions of the monochromator scan and EDD methods, it combines the convenience of easy peak indexing and unit-cell parameter determination with very short readout times, and offers the possibility for time-resolved studies. Modern and revised ideas of applying foil-mask spectroscopy in LD experiments are presented elsewhere in this volume (Hanley & Denton, 2005).

There is an additional possibility of producing a pink beam by the use of a multilayer as monochromator. Such a device has $E/\Delta E \simeq 100$ and thus could be a fast and convenient alternative to the foil-mask technique (Kunz, 2005).

6.4. Sample rotation and absorption-edge detection spectroscopy

Although the fact that the sample does not have to be rotated was emphasized as one of the great advantages of Laue diffraction, if no other way of determining peak energies is available, sample rotation can be used to deal with that problem by recording oscillation Laue images and detecting the presence of the absorption edge of the foil. Details of the peak energy determination method based on sample rotation are described elsewhere (Dera, 2005).

7. Structure factor amplitude determination

As indicated earlier, pSXD experiments for materials research typically measure known crystal structures. In order to determine details of the atomic arrangement within the unit cell it is necessary to obtain precise structure factor amplitude information, which comes from the measurement of the reciprocal-space integrated intensities. In a monochromatic experiment, all reflections utilize the same incident intensity and wavelength (or the time-dependence of the incident intensity is monitored and easily taken into account). Absorption effects caused by the sample itself, the air or the presence of the DAC are dependent only on the length of the beam path through each medium. The case is much more complicated for polychromatic diffraction. In a polychromatic Laue image the measured peak intensities are affected by: (i) different peak energies through the Darwin equation ($I \simeq 1/E^3$), (ii) incident-beam energy spectrum [$I \simeq I_0(E)$], (iii) harmonic overlaps, (iv) absorption phenomena with energy-dependent X-ray attenuation coefficients, and (v) energy dependence of detector efficiency.

Protein Laue crystallography has developed methods to numerically determine most of the above-described corrections; however, these methods depend strongly on the following assumptions: (*a*) the availability of a large number of observations, which are not typically available for small unit-cell crystals, (*b*) a knowledge of the unit-cell parameters and (*c*) no absorbing sample enclosure.

Several encouraging pSXD test studies have been performed with small unit-cell volume crystals. Euler *et al.* (1994) determined the orientation and refined unit-cell parameters for the olivine $Mg_{90}Fe_{10}SiO_4$ crystal, Kariuki & Harding (1995) determined the structure of inorganic salts $PbCO_3$, $SrCo_3$ and $Cu_2(OH)_2CO_3$ by Patterson analysis, Ravelli *et al.* (1999) solved structures of molecular crystals $C_{40}H_{46}N_4O_{14}$, $C_{10}H_{14}O_2$ and $C_{18}H_{19}N_3O_2$ *via* direct methods, and Dodd *et al.* (1994) refined the structure of an organometallic compound containing anomalously scattering atoms $[AuOs_3H(CO)_8\{Ph_2PCH_2P(Ph)C_6H_4\}(PPh_3)]PF_6{\cdot}0.5C_6H_5Cl$.

While these successful experiments prove that crystals with small unit cells can be dealt with using the LD technique, the use of the DAC further complicates most of the corrections, and custom modifications to the standard LD methods are needed.

7.1. Energy spectrum of the incident beam

The energy spectra $I_0(E)$ of a white beam depends on the beamline source and on the beamline transport optics. Szebenyi *et al.* (1992) and Šrajer *et al.* (2000) demonstrated that, even for incident spectra exhibiting very complex functional form such as those produced by undulator and wiggler insertion devices, with sufficient redundancy of the experimental observations it is possible to properly normalize the incident spectrum with the use of Chebyshev polynomials. For experiments in DAC, normalization based entirely on the single Laue pattern would be very difficult because of the additional intensity-affecting phenomena; however, the ultrafast crystal oscillation technique, described by Dera (2005), can be conveniently applied. Recently, more and more modern synchrotron facilities have been switching to operation in the top-up mode, in which the time-dependence of the incident intensity and incident spectrum are minimal. In such cases a whole series of Laue images can be processed with the same normalization function.

7.2. Energy-dependence of the detector sensitivity

The detector response to diffracted radiation depends strongly on the wavelength of the diffracted beams. If the only detector available in the experiment is the area detector used to collect Laue images, then the detector sensitivity is inseparable from the incident beam energy spectrum, and the two effects can be treated together. The combined effect can be described by function $I_d(E) = I_0(E)\,D_s(E)$.

7.3. Energy-dependence of absorption along the beam path

Both the incident and the diffracted beams travel through a range of different media, including air, the sample, parts of the DAC, and the pressure-transmitting medium before they hit the active element of the detector. Since the X-ray attenuation coefficient of every substance exhibits energy dependence, peaks with different energies will be affected by absorption to a different degree. In order to properly account for the absorption effects, the beam path has to be reconstructed and its length through each medium properly modeled or experimentally measured. The length of the path of the incident beam through the air, before entering the DAC, is more or less constant for all reflections and all sample orientations, and its effect is inseparable from I_d. The remaining absorption effects can be described by the following equation,

$$T = \exp\left[-\mu_B\left(l_B^1 + l_B^1\right) - \mu_D\left(l_D^1 + l_D^2\right) - \mu_H\left(l_H^1 + l_H^2\right) - \mu_S l_S - \mu_A l_A - \mu_P l_P\right].$$

Here subscripts correspond to the following media: B, backing plate; D, diamond; H, hydrostatic medium; S, sample; A, air; P, phosphor material; and superscripts 1 and 2 correspond to the incident and diffracted beam, respectively. The values of path length l for each medium depend on the particular experimental setup and type of the DAC used.

7.4. Presence of multiple harmonics

In Laue diffraction, multiple wavelength components may be present along the same diffracted beam direction. Since these components correspond to different structure factors, the deconvolution of the harmonics and determination of proper partitioning of the observed intensity between different structure factors is critical from the point of view of structure solution and refinement. Usually as many as 20% of the observed peaks have at least two harmonic components. Several purely numerical methods have been developed to deal with the harmonic overlap problem. Hao *et al.* (1993, 1995) and Campbell & Hao (1993) introduced a deconvolution method based on analysis of the direct space Patterson function calculated assuming that all the reflections are singlets.

Bourenkov *et al.* (1996) introduced statistical methods for harmonic decomposition, which implements a Bayesian approach and does not require high redundancy in the measurement. Ren & Moffat (1995) utilized a wavelength-normalization method based on Laue spots measured at different energies. In high-pressure LD experiments, the additional intensity-affecting factors, described above, make the computational approaches less effective, and experimental solutions should be considered.

Three major experimental methods for harmonic deconvolution can be distinguished, as follows.

7.4.1. Monochromatic scan method. In principle, the monochromator scan method deconvolutes the harmonic overlaps directly. However, in practice, additional difficulties need to be faced. The first problem is proportionality of the incident intensity of the monochromated beam to the intensity of the equivalent-energy component of the white beam, $I_0^{\rm m}(\lambda) = f_{\rm p\rightarrow m}(\lambda) I_0^{\rm p}(\lambda)$. With a submicrometre-sized beam, even small displacements of the beam during scanning can introduce intensity-affecting misalignments. During preliminary measurements on 34-ID-E, the monochromator position was manually realigned every 2 keV to optimize the intensity output. A feedback system for monochromator position adjustment exhibiting high efficiency, fast response and yielding reproducible results will be a key component of a microdiffraction system designed for high-pressure applications. Because of this monochromator misalignment problem, the energy scans are usually performed in a step, rather than in a continuous manner (*i.e.* the monochromator is still during exposure), whereas it would be optimal to utilize narrow-bandpass pink radiation rather than pure monochromatic radiation. In order to properly partition the intensity between the different energy components of a reflection, the measured intensities obtained from the monochromator scan, $I_{hkl}^{\rm m}(\lambda_i)$, for the same diffracted beam must be scaled by $f_{\rm p\rightarrow m}^{-1}(\lambda_i)$. Because of the duration of a fine energy scan it is usually not convenient to cover a wide enough energy range to record multiple harmonics, especially in the higher-energy region. However, if a single energy component $I_{hkl}^{\rm m}(\lambda_1)$ of a diffracted beam is detected, the presence of other harmonic components can be first verified either by examination of the relation $I_{hkl}^{\rm m} f_{\rm p\rightarrow m}^{-1}(\lambda_i) = I_{hkl}^{\rm p}$, and, if the latter is not satisfied, by recording monochromatic images at exactly $\lambda_j = n\lambda_i$.

7.4.2. Foil-mask spectrometer method. The foil-mask spectrometer method, described above for the peak energy determination, can be used for harmonic decomposition, as described by Hanley *et al.* (1997), utilizing the fact that each of the harmonic components, having different energy, is affected differently by an absorption foil placed in the incident beam.

7.4.3. Absorption-edge detection (AED) method. The AED method (Dera, 2005) takes advantage of the same energy-dependence of X-ray attenuation coefficient, but utilizes sample rotation during exposure. The peak energy is determined by detecting the discontinuous peak intensity drop corresponding to an absorption edge. The AED method also allows for convenient deconvolution of harmonic overlaps.

8. Pilot experiments

To test the monochromator scan approach to high-pressure experiments, we performed an exploratory series of experiments on the polychromatic microdiffraction station 34-ID-E at the Advanced Photon Source.

8.1. Sample preparation

A small 20 µm × 20 µm × 5 µm crystal of synthetic (Aldrich) chromite $FeCr_2O_4$ was placed in a panoramic DAC. The diamond anvils used had culets of 0.4 mm and were mounted on tungsten backing plates with conical access holes. A Be foil with initial thickness 0.5 mm and hole diameter 0.2 mm was used as a gasketing material. The gasket hole was filled with He as the pressure-transmitting medium. Small ruby chips placed in the gasket hole were used for pressure calibration. For data collection the sample was at a pressure of 10 GPa. The DAC was mounted inside a motorized χ-rotation stage which allows cell rotations about the incident beam. A schematic of the experimental setup is shown in Fig. 7. The cell was centered inside the χ stage to preserve the sample position during rotations.

8.2. Experimental alignment

Since our experiment was the first DAC data collection attempted on ID-34-E, modifications of the standard setup were necessary. For materials experiments, the axis of the sample alignment microscope is approximately normal to the sample surface which bisects the nominal $2\theta \simeq 90^\circ$ scattering angle of the detector. This geometry excludes optical access to the DAC sample. To allow for optical alignment we used an off-line microscope with known translational offset between the off-line microscope cross-hair and the incident beam at the data collection position. The whole *XYZ* translation stage with the DAC on the top was first optically aligned off-line. The

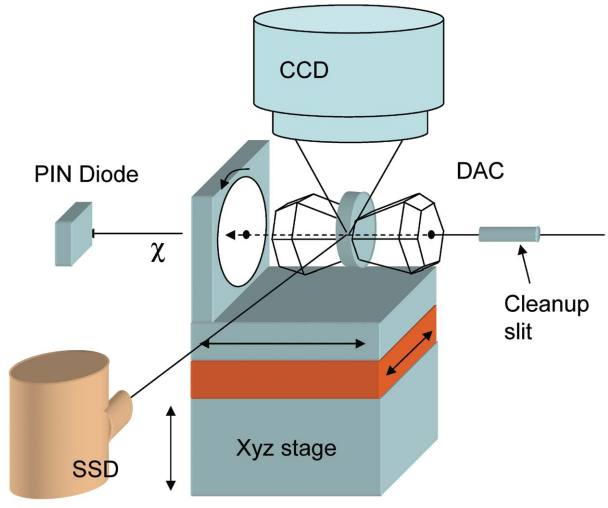

Figure 7
Experimental setup for prototype high-pressure polychromatic microdiffraction experiment. The stage was moved off-line with the DAC for rough alignment with an optical microscope.

precalibrated stage was then moved to the data collection position for fine sample centering.

In DAC experiments with X-ray opaque gaskets, usually the contrast in X-ray beam transmittance between the gasket hole inside and outside is used for fine alignment (measured with a pin diode detector). However, with Be gaskets the contrast is insufficient, and alternative alignment methods are necessary. Since the sample contained Cr, which produces strong fluorescence, we used a solid-state Ge detector to detect sample coincidence with the beam (Another possible solution is to use a very low energy beam, ~5–8 keV, and the conventional X-ray absorption contrast technique.)

The diffraction data were collected by a fast Roper Scientific 16-bit 2k × 2k CCD X-ray-sensitive area detector placed 45 mm from the sample. After locating the sample position with fluorescence we performed a two-dimensional grid scan with range 100 μm × 100 μm, collecting Laue images at each step. Fig. 8 shows Laue images with the incident beam illuminating the sample (Figs. 8*a* and 8*b*) and passing 20 μm away from the sample (Figs. 8*c* and 8*d*). The reflections common in the two images are from diamond anvils. In a single Laue image, ~50 sample reflections could be located.

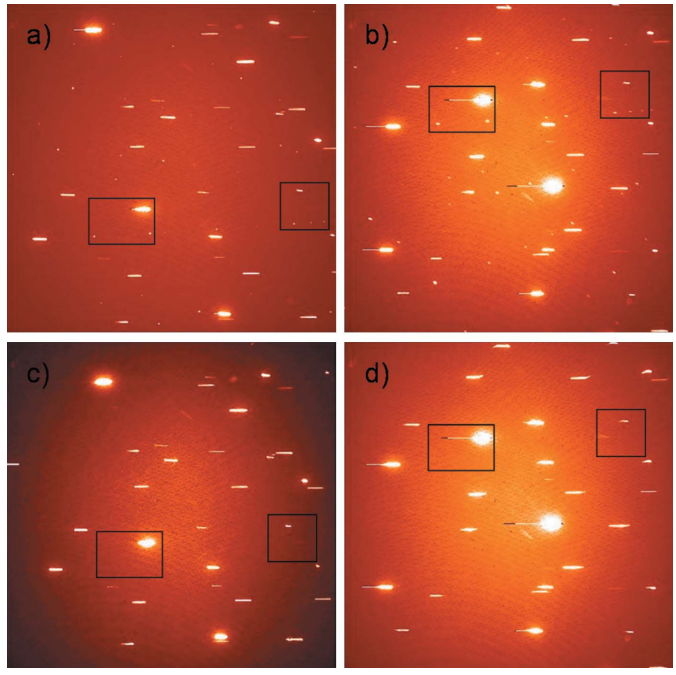

Figure 8
Laue patterns with the incident beam illuminating the sample (*a* and *b*) and passing through the gasket hole away from the sample (*c* and *d*). Images (*a*) and (*c*) are taken at $\chi = 0°$, images (*b*) and (*d*) at $\chi = 20°$.

8.3. Monochromatic data collection

In order to determine peak energies for the observed Laue spots, we performed an energy scan in the range 15–20 keV with 10 eV steps (500 images) and 10 s exposure time, at $\chi = 0$. The incident spectrum range for white beam was approximately 5–25 keV. When the scan was completed we examined all the monochromatic images for the presence of reflections corresponding to the Laue spot coordinates. A peak-fitting procedure was performed to precisely determine the reflection energy for Laue spots that fell within the energy range of the scan. The average energy full-width-at-half-maximum was ~50 eV, and peaks were usually recorded in five consecutive images. In the scanned energy range, 12 of the ~50 Laue reflections were found. Based on these 12 reflections, the orientation matrix was calculated and the unit-cell parameter was determined to be 8.230 (5) Å. The value of the lattice parameter we obtained is in good agreement with the bulk modulus value (197 GPa) determined by White *et al.* (2005). Analysis of the intensity data for the chromite sample is underway and will be presented in a separate paper.

9. Summary and future prospects

High-pressure crystallography is in a desperate need of novel methodological approaches, which could overcome the obstacles imposed by the use of diamond anvil cells. Emerging polychromatic microdiffraction techniques developed for protein crystallography and materials science address most of the problems that have been holding back single-crystal diffraction at high pressure. Limitations intrinsic to standard Laue diffraction, and relevant for high-pressure applications, such as undetermined peak energies, harmonic overlaps and reciprocal space access restrictions can be resolved with experimental modifications, discussed above. However, since the modified methodology is not standard, and neither optimized hardware setups nor appropriate software currently exist, a focused developmental effort located at high-pressure synchrotron beamlines will be needed. On the other hand, many of the solutions and modifications motivated by the specific needs of high-pressure experiments will be of great benefit to non-high-pressure applications of polychromatic diffraction. pSXD development efforts have been initiated at several beamlines in the USA: HPCAT, UNICAT and GSECARS at APS, stations X17B and X17C at NSLS, and station 12.2.2 at ALS.

The authors would like to thank J. Shu of Geophysical Laboratory for help with sample preparation, and W. Yang of UNICAT for help with data collection. The authors acknowledge support from NSF, through grant EAR-0217389. This work was also sponsored in part by the Division of Materials Sciences and Engineering Office of Basic Energy Sciences through contract DE-AC05-00OR22725 with the Oak Ridge National Laboratory (ORNL), which is operated by UT-Battelle, LLC, for the US Department of Energy. Experiments were performed on UNICAT beamline 34-ID at the Advanced Photon Source, Argonne, IL. Both 34-ID and the APS are funded by the DOE Office of Basic Energy Science. The submitted manuscript has been authored by a contractor of the US Government under contract No. DE-AC05-00OR22725. Accordingly, the US Government retains a nonexclusive royalty-free license to publish or reproduce the published form of this contribution, or allow others to do so,

for US Government purposes The authors would like to thank John B. Parise and Martin Kunz for valuable comments and suggestions regarding improvement of the manuscript.

References

Barabash, R. I., Ice, G. E. & Pang, J. W. L. (2005). *Mater. Sci. Eng. A*. In the press.

Barabash, R. I., Ice, G. E., Tamura, N., Valek, B. C., Bravman, J. C., Spolenak, R. & Patel, J. R. (2004). *Microelectron. Eng.* **75**, 24–30.

Bourenkov, G. P., Popov, A. N. & Bartunik, H. D. (1996). *Acta Cryst.* A**52**, 797–811.

Budai, J. D., Yang, M., Larson, B. C., Tischler, J. Z., Liu, W., Weiland, H. & Ice, G. E. (2004). *Mater. Sci. Forum*, **467/470**, 1373–1378.

Budai, J. D., Yang, W. G., Tamura, N., Chung, J. S., Tischler, J. Z., Larson, B. C., Ice, G. E., Park, C. & Norton, D. P. (2003). *Nature Mater.* **2**, 487–492.

Campbell, J. W. & Hao, Q. (1993). *Acta Cryst.* A**49**, 889–893.

Carr, P. D., Cruickshank, D. W. J. & Harding, M. M. (1992). *J. Appl. Cryst.* **25**, 294–308.

Chung, J.-S. & Ice, G. E. (1999). *J. Appl. Phys.* **86**, 5249–5255.

Cole, J. M., McIntyre, G. J., Lehmann, M. S., Myles, D. A. A., Wilkinson, C. & Howard, J. A. K. (2001). *Acta Cryst.* A**57**, 429–434.

Cruickshank, D. W. J., Helliwell, J. R. & Moffat, K. (1991). *Acta Cryst.* A**47**, 352–373.

Dera, P. (2005). In preparation.

Dera, P., Downs, R. T. & Somayazulu, M. (2005). In preparation.

Dodd, I. M., Hao, Q., Harding, M. R. & Prince, S. M. (1994). *Acta Cryst.* B**50**, 441–447.

Euler, H., Gilles, R. & Will, G. (1994). *J. Appl. Cryst.* **27**, 190–192.

Finger, L. W. & King, H. (1978). *Am. Mineral.* **63**, 337–342.

Hanley, Q. S., Campbell, J. W. & Denton, M. B. (1997). *J. Synchrotron Rad.* **4**, 214–222.

Hanley, Q. S. & Denton, M. B. (2005). *J. Synchrotron Rad.* **12**, 618–625.

Hanley, Q. S., Dunphy, D. R. & Denton, M. B. (1996). *J. Synchrotron Rad.* **3**, 101–111.

Hao, Q., Campbell, J. W., Harding, M. M. & Helliwell, J. R. (1993). *Acta Cryst.* A**49**, 528–531.

Hao, Q., Harding, M. M. & Campbell, J. W. (1995). *J. Synchrotron Rad.* **2**, 27–30.

Ice, G. E., Barabash, R. I. & Liu, W. (2005). *Z. Mater.* In the press.

Ice, G. E., Chung, J.-S., Tischler, J. Z., Lunt, A. & Assoufid, L. (2000). *Rev. Sci. Instrum.* **71**, 2635–2639.

Ice, G. E., Larson, B. C., Yang, W., Budai, J. D., Tischler, J. Z., Pang, J. W. L., Barabash, R. I. & Liu, W. (2005). *J. Synchrotron Rad.* **12** 155–162.

Kariuki, B. M. & Harding, M. M. (1995). *J. Synchrotron Rad.* **2**, 185–189.

Kim-Zajonz, J., Werner, S. & Schulz, H. (1998). *Z. Krystallogr.* **214**, 331–336.

Kingma, K. J., Cohen, R. E., Hemley, R. J. & Mao, H. K. (1995). *Nature (London)*, **374**, 243–245.

Kunz, M. (2005). Private communication.

Larson, B. C., Yang, W., Ice, G. E., Budai, J. D. & Tischler, J. Z. (2002). *Nature (London)*, **415**, 887–890.

Liu, J. & Vohra, Y. K. (1996). *Appl. Phys. Lett.* **68**, 2049–2051.

Loubeyre, P., LeToullec, R., Hausermann, D., Hanfland, M., Hemley, R. J., Mao, H. K. & Finger, L. W. (1996). *Nature (London)*, **383**, 702–704.

Mao, H. K. & Bell, P. M. (1978). *Science*, **200**, 1145–1147.

Mao, H. K., Shu, J., Hu, J. & Hemley, R. J. (1994). *Eos, Trans. Am. Geophys. Union*, **75**, 662.

Mao, H. K., Shu, J., Shen, G., Hemley, R. J., Li, B. & Singh, A. K. (1998). *Nature (London)*, **396**, 741–743.

Miletich, R., Allan, D. R. & Kuhs, W. F. (2000). In *High-Temperature and High-Pressure Crystal Chemistry, Reviews in Mineralogy and Geochemistry*, Vol. 41, edited by R. M. Hazen and R. T. Downs. Washington, DC: MSA.

Pan, J. (1992). *J. Appl. Cryst.* **25**, 195–198.

Pang, J. W. L., Ice, G. E. & Liu, W. (2005). *Acta Mater.* Submitted.

Ravelli, R. B. G., Hezemans, A. M. F., Krabbendam, H. & Kroon, J. (1996). *J. Appl. Cryst.* **29**, 270–278.

Ravelli, R. B. G., Raves, M. L., Scheres, S. H. W., Schouten, A. & Kroon, J. (1999). *J. Synchrotron Rad.* **6**, 19–26.

Ren, Z., Bourgeois, D., Helliwell, J. R., Moffat, K., Šrajer, V. & Stoddard, B. L. (1999). *J. Synchrotron Rad.* **6**, 891–917.

Ren, Z. & Moffat, K. (1994). *J. Synchrotron Rad.* **1**, 78–82.

Ren, Z. & Moffat, K. (1995). *J. Appl. Cryst.* **28**, 482–493.

Sheremetyev, I. A. & Gorfman, S. (2001). *Nucl. Instrum. Methods A*, **470**, 223–227.

Šrajer, V., Crosson, S., Schmidt, M., Key, J., Schotte, F., Anderson, S., Perman, B., Ren, Z., Teng, T. Y., Bourgeois, D., Wulff, M. & Moffat, K. (2000). *J. Synchrotron Rad.* **7**, 236–244.

Szebenyi, D. M. E., Bilderback, D., LeGrand, A., Moffat, K., Schildkamp, W., Temple, B. S. & Teng, T. Y. (1992). *J. Appl. Cryst.* **25**, 414–423.

Tamura, N., MacDowell, A. A., Spolenak, R., Valek, B. C., Bravman, J. C., Brown, W. L., Celestre, R. S., Padmore, H. A., Batterman, B. W. & Patel, J. R. (2003). *J. Synchrotron Rad.* **3**, 101–111.

Wenk, H. R., Heidelbach, F., Chateigner, D. & Zontone, F. (1997). *J. Synchrotron Rad.* **4**, 95–101.

White, A., Ma, Y., Aksoy, R., Selvi, E. & Sandhu, J.-S. (2005). *SMEC 2005 – Study of Matter at Extreme Conditions*, 17–21 April 2005, Miami, USA. Meeting Abstracts.

Yamanaka, T., Fukuda, T. & Tsuchiya, J. (2001). *Phys. Chem. Miner.* **29**, 633–641.

Zhang, L. & Ahsbahs, H. (1998). *Rev. High. Press. Sci. Technol.* **7**, 145–147.

Zhang, L., Ahsbahs, H. & Kutoglu, A. (1998). *Phys. Chem. Miner.* **25**, 301–307.